



Photoluminescence decay time measurements from self-organized InAs/GaAs quantum dots

P. D. Buckle, P. Dawson, S. A. Hall, X. Chen, M. J. Steer, D. J. Mowbray, M. S. Skolnick, and M. Hopkinson

Citation: *Journal of Applied Physics* **86**, 2555 (1999); doi: 10.1063/1.371092

View online: <http://dx.doi.org/10.1063/1.371092>

View Table of Contents: <http://scitation.aip.org/content/aip/journal/jap/86/5?ver=pdfcov>

Published by the [AIP Publishing](#)



Re-register for Table of Content Alerts

Create a profile.



Sign up today!



Photoluminescence decay time measurements from self-organized InAs/GaAs quantum dots

P. D. Buckle, P. Dawson,^{a)} S. A. Hall, and X. Chen
*Department of Physics, University of Manchester Institute of Science and Technology, P.O. Box 88,
Manchester, M60 1QD United Kingdom*

M. J. Steer, D. J. Mowbray, and M. S. Skolnick
Department of Physics, University of Sheffield, Sheffield, S3 7RH United Kingdom

M. Hopkinson
*EPSRC Central Facility for III–V Semiconductors, Department of Electronic and Electrical Engineering,
University of Sheffield, Sheffield, S1 3JD United Kingdom*

(Received 2 November 1998; accepted for publication 3 June 1999)

In this article we report the results of time integrated and time resolved photoluminescence spectroscopy and photoluminescence time decay measurements as a function of excitation density at 6 K on high quality self-organized InAs/GaAs quantum dots. To understand the form of the experimentally observed photoluminescence transients a Monte Carlo model has been developed that allows for the effects of random capture of photo-excited carriers. By comparison with the results of our model we are able to ascribe the excitation density dependence of the overall form of the decay of the emission from the quantum dot ground states and the biexponential nature of the decay of the first excited state emission as being due to the combined effects of radiative recombination, density dependent carrier scattering, and the restriction of carrier scattering due to state blocking caused by the effects of Pauli exclusion. To successfully model the form of the biexponential decay of the highest energy excited states we have to invoke the nonsequential scattering of carriers between the quantum dot states. © 1999 American Institute of Physics. [S0021-8979(99)08817-9]

I. INTRODUCTION

Detailed understanding of the Stranski–Krastanov coherent island growth mode (self-organized growth) has allowed the fabrication of high optical quality nanometer sized quantum dots.^{1,2} Under certain growth conditions the formation of pyramidal InAs quantum dots on epitaxially grown GaAs has been observed,^{1–3} similar behavior has also been observed in other material systems for which there is sufficient lattice mismatch.^{4,5} Quantum dots provide a zero-dimensional system, with three-dimensional carrier confinement resulting in atomic-like, discrete electronic eigenstates. The δ -like density of states and predicted⁶ large oscillator strengths are anticipated to lead to improved opto-electronic device behavior. In particular, the most important of which are likely to be the lowering of the laser threshold current densities,^{7,8} and higher values⁹ of T_0 compared with existing semiconductor lasers.

Central to the use of quantum dots in opto-electronic devices is the question of carrier relaxation, since it is expected that the existence of discrete, atomic-like energy levels may prevent efficient phonon assisted carrier scattering, the so-called “phonon bottleneck.”¹⁰ Originally the phonon bottleneck was held to be responsible for the low photoluminescence efficiencies of quantum dots fabricated by lithographic techniques.¹⁰ However, quantum dots fabricated using the Stranski–Krastanov technique exhibit high

photoluminescence efficiencies^{11,12} at low temperatures, suggesting that the reduced carrier scattering rates do not intrinsically lead to poor photoluminescence efficiency. Furthermore, lasing has now been achieved in self-organized quantum dot structures,^{13,14} and so clearly the investigation of carrier relaxation in these quantum dots is important. The most widely studied self-organized quantum dot system is InAs/GaAs which has provided a model system for the study of carrier capture, carrier scattering, and recombination dynamics.^{15–27} It has been proposed that carrier relaxation within quantum dots occurs via Auger scattering^{16,22–24,28} or multiphonon processes.^{15,25,26,29} One distinguishing feature of quantum dot systems is that carrier relaxation rates can also be influenced by state blocking effects, due to Pauli exclusion, when the lower states are full. This has been demonstrated at excitation densities such that the multiple carrier occupation of the quantum dots is achieved.^{17,30} The majority of the experimental data reported so far has been analyzed by rate equation approaches where the effects of state blocking are difficult to incorporate. Of particular relevance to the analysis of recombination dynamics is the work of M. Grundmann and D. Bimberg³¹ who demonstrate that due to the random nature of the carrier capture by the quantum dots significant excited state emission intensity can be observed even at photoexcited carrier densities significantly less than the areal density of the quantum dots. Again these effects are difficult to include in a rate equation analysis of the carrier dynamics.

^{a)}Electronic mail: philip.dawson@umist.ac.uk

In this article we present a study of the carrier recombination and scattering dynamics in self-organized InAs/GaAs quantum dots, using continuous wave and time resolved photoluminescence spectroscopy and time decay photoluminescence measurements. To analyze the data we have developed a Monte Carlo model that allows the random nature of the carrier capture process by the quantum dots to be taken into account as well as the significant effects of state blocking. The use of this model is shown to be critical in determining the relative contributions of the different recombination and scattering mechanisms.

II. EXPERIMENTAL DETAILS

The samples were grown by solid source molecular-beam epitaxy under conditions similar to those of Moison *et al.*¹ The sample structure consisted of an undoped GaAs substrate on which was grown a GaAs buffer layer, followed by a thin layer of InAs nominally 2.4 monolayers (ML) thick grown at a rate of 4 ML per second. X-ray analysis of samples containing InGaAs/GaAs multiple quantum well structures, used as a reference, suggested that the InAs thickness may be 5%–10% lower than intended due to In desorption at the growth temperature used ($T_g = 500\text{--}520^\circ\text{C}$). The resulting quantum dots have a base length ~ 12 nm and height ~ 3 nm, and density $\sim 1 \times 10^{11} \text{ cm}^{-2}$ as confirmed by plan view and cross-sectional transmission electron microscopy. The growth was terminated with the InAs quantum dots being overgrown by a GaAs capping layer with a thickness of 100 nm.¹²

For the photoluminescence decay time measurements the sample was excited by a mode locked, cavity dumped dye laser (output wavelength = 5825 Å) operating at a repetition rate of 3×10^5 Hz with a pulse width ≤ 10 ps. The technique of time correlated single photon counting was used to process the signal detected by a cooled S1 microchannel plate via a 0.85 m grating spectrometer. The temporal resolution of this system was approximately 70 ps.

Time integrated photoluminescence spectra were obtained by exciting the structure with chopped light from the mode locked dye laser. The resultant emission was dispersed by the 0.85 m single grating spectrometer and detected with a liquid nitrogen cooled Ge *p-i-n* photodiode followed by a lock-in detector.

For all the optical experiments the sample was mounted on the cold finger of a variable temperature (6–300 K) closed cycle helium cryostat.

III. RESULTS & DISCUSSION

A. Time integrated photoluminescence spectroscopy

Shown in Fig. 1 are the time integrated photoluminescence spectra measured at 6 K using a range of incident photon excitation densities. The excitation densities quoted are the incident photon densities per laser pulse and not carrier densities since it is difficult to be precise about the density of electron/hole pairs captured by the quantum dots due to the effects of radiative and nonradiative recombination in the GaAs and the wetting layer before carrier capture. However, it is reasonable to assume that for the range of excita-

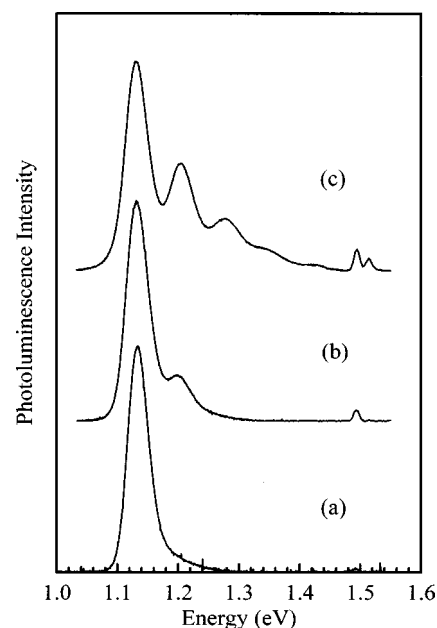


FIG. 1. Time integrated photoluminescence spectrum for excitation photon densities per pulse of (a) $3 \times 10^9 \text{ cm}^{-2}$, (b) $8 \times 10^{12} \text{ cm}^{-2}$, and (c) $2 \times 10^{14} \text{ cm}^{-2}$.

tion densities used ($3 \times 10^9 \text{ cm}^{-2} \rightarrow 2 \times 10^{14} \text{ cm}^{-2}$) we cover the range of average carrier densities captured by the quantum dots from less than one electron/hole pair per quantum dot to greater than one electron/hole pair per quantum dot.

The spectrum recorded at the lowest excitation density [Fig. 1(a)] has a single feature, with a peak energy of 1.131 eV, which has been ascribed previously¹² to recombination involving carriers in the lowest energy confined electron and hole states (designated as ground state recombination). As the excitation density is increased, features at a higher energy appear in the spectra at 1.205, 1.277, and 1.345 eV. These peaks have been attributed¹² to the recombination from excited states of the quantum dots. For the purposes of this article the precise nature of the electron and hole states involved in the ground state and excited state recombination are not particularly relevant and we treat the quantum dots as having four optically active excitonic states, i.e., a ground state and three excited states.

Previous studies¹² of the same sample using photoluminescence excitation spectroscopy has identified the photoluminescence peak at 1.420 eV as being due to interband transitions in the InAs wetting layer. The peaks at 1.515 and 1.494 eV are due to recombination involving bulk GaAs free excitons and GaAs acceptors.

B. Photoluminescence time decay measurements

1. Ground state recombination

Shown in Fig. 2 are the results of photoluminescence time decay measurements obtained whilst detecting on the peak of the ground state emission (1.131 eV) for the various excitation densities corresponding to the time integrated photoluminescence spectra of Fig. 1. As the excitation density is increased a gradual change occurs in the form of the photoluminescence transient. For the lowest excitation density

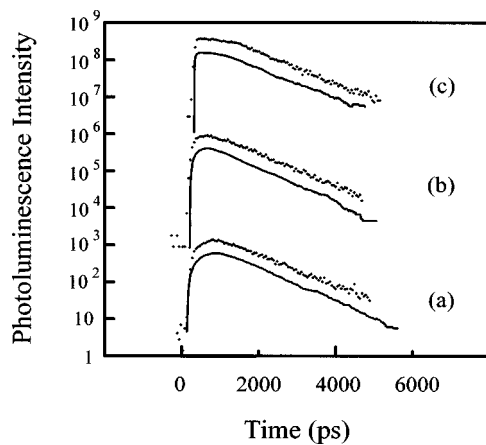


FIG. 2. The results (\cdots) of experimental photoluminescence time decay measurements while monitoring the ground state emission (detection energy = 1.131 eV) for excitation photon densities per pulse of (a) $3 \times 10^9 \text{ cm}^{-2}$, (b) $8 \times 10^{12} \text{ cm}^{-2}$, and (c) $2 \times 10^{14} \text{ cm}^{-2}$. The solid lines are the results of Monte Carlo simulations for the decay of the ground state population for injected reservoir carrier densities of (a) $1 \times 10^{10} \text{ cm}^{-2}$, (b) $1.3 \times 10^{11} \text{ cm}^{-2}$, and (c) $1.3 \times 10^{12} \text{ cm}^{-2}$. The experimental results and the simulation results are offset for clarity.

[Fig. 2(a)] the rise of the photoluminescence is initially rapid, but then slows, reaching a peak after ~ 800 ps. The photoluminescence intensity then falls, tending to a single exponential decay at times greater than 2000 ps with a characteristic time constant of 1.0 ns. For a higher excitation density [Fig. 2(b)] the rise of the photoluminescence intensity is more rapid, with the maximum photoluminescence intensity occurring after ~ 500 ps. However, after 2000 ps a single exponential decay with a time constant of 1.0 ns is observed. For the highest excitation density used [Fig. 2(c)] the onset of the photoluminescence is now dominated by a fast rise with the photoluminescence intensity reaching a maximum in a time determined by the response of the measurement system (~ 70 ps). The photoluminescence intensity then remains approximately constant, forming a plateau for approximately 1000 ps, before once more tending to a single exponential decay with a time constant of 1.0 ns.

In order to understand the form of these transients we need to consider the mechanisms by which carriers can relax within the quantum dots. Initially the majority of the photoexcited electron-hole pairs are created in the GaAs from which they are rapidly captured by the quantum dots, either directly or via the InAs wetting layer, on a time scale ~ 50 ps.³² Once the carriers are captured by the quantum dots it is generally assumed that they subsequently relax sequentially via the excited states to the ground state. An analytical rate analysis for sequential carrier relaxation has been performed by Adler *et al.*¹⁶ In this rate equation model it is assumed that all the optically excited carriers are captured rapidly into the highest energy quantum dot state, followed by sequential scattering only into the next lowest energy confined state, forming a ‘‘ladder’’ type relaxation path to the ground states of the quantum dots. Although the ground state photoluminescence transient shown in Fig. 2(a) (low excitation density) can be modeled using such a rate analysis with appropriate filling and recombination rates, using the same

approach for the modeling of the high excitation density transients in Figs. 2(b) and 2(c) tends to be somewhat more problematic. In particular, an analytical approach based on rate equations has serious limitations³¹ as Pauli state blocking effects which prevent relaxation to a lower fully occupied level are difficult to incorporate.

Therefore, in this work we have used a Monte Carlo model to describe the dynamics of the quantum dots, such a treatment allows the effects of state blocking to be dealt with more rigorously. Another advantage of a Monte Carlo treatment is that we can easily incorporate the random nature of carrier capture by the quantum dots, which is extremely important, as noted by M. Grundmann and D. Bimberg.³¹ This is achieved by allowing carriers to be captured by the quantum dots from a reservoir rather than starting with initial conditions where the highest excited state is full. An important input parameter of our model is the carrier density at $t = 0$ in the injection reservoir. This provides a more physically realistic situation than assuming that the highest quantum dot states are occupied at $t = 0$.

For our Monte Carlo simulation we use a 50 000 element array to simulate the quantum dots containing four optically active states. We note that the degeneracies of the quantum dot states appear to increase with increasing index, as reflected³³ by the increasing maximum emission intensity as a function of the excited state index. Clearly the degeneracies of the states depend on the precise nature of the confined electronic states. As this is still the cause of a great deal of uncertainty we emphasize that the overall conclusions reached in this article are not, to any great extent, influenced by the assumed degeneracies. In practice the effects arising from varying the assumed degeneracies can be countered by varying the density of carriers in the injection reservoir.

The input parameters of our model are as follows. At $t = 0$ the number of carriers in the reservoir is defined along with a scattering time of 50 ps³² for carrier capture into the highest energy excited states. Probabilities per unit time representing scattering between individual quantum dot states are also defined, as are probabilities for parallel loss processes representing radiative decay from each individual quantum dot state. Using the terminology τ_{x-y} where x is the index of the higher energy excited state and y is the index of the next lowest energy state, scattering times of $\tau_{4-3} = 180$ ps, $\tau_{3-2} = 200$ ps, and $\tau_{2-1} = 260$ ps along with radiative lifetimes of 1, 3.7, 1.6, and 1.2 ns for carriers in the ground, first excited, second excited, and third excited states, respectively, were used in the model to obtain good fits to the experimental data. The scattering times τ_{x-y} used in the model are compatible with those expected for acoustic phonon scattering²⁸ where the energy separation between the electronic states is large. The values quoted are somewhat less than those extracted from the work of Adler *et al.*¹⁶ and considerably greater than those used in the work of Heitz *et al.*¹⁵ The reason for this discrepancy may be that the values quoted in the previous work^{15,16} were extracted from experimental data where the strong excited state emission was observed in the photoluminescence spectra suggesting a high excitation power density. As discussed later, at high excitation carrier densities Auger processes can lead to en-

hanced scattering rates that can be shorter than the acoustic phonon scattering rates, this may be the reason for the differences in the published scattering rates and those used in this article. We stress that the quoted scattering rates are extracted from comparison with experimental data obtained under conditions when it is reasonable to assume that Auger enhanced scattering does not occur.

Due to the high radiative efficiency of the quantum dots¹² it is assumed that interlevel scattering and radiative decay are the only processes that determine the dynamics of the quantum dot states. Auger scattering is simulated by enhancing the scattering probabilities as a function of the number of carriers remaining in the injection reservoir. These rates are taken directly from the theoretical work of U. Bocklemann and T. Egeler.²⁴ Auger enhanced scattering, which is only relevant for high carrier densities in the reservoir, occurs on a very short time scale which is faster than the experimental system response. Thus, the precise form of the carrier density dependence of the Auger scattering rate is relatively unimportant when modeling the carrier dynamics. The scattering and radiative loss probabilities for each state, together with capture probabilities for carriers injected from the reservoir form the input parameters to the simulation. Random scattering events for each individual carrier are then generated and the program is iterated until all carriers have been lost (all quantum dots empty). The only modification to the scattering probabilities during the course of the simulation occurs when the probability for carrier scattering between two states is set to zero if the lowest state is fully occupied, hence, reflecting the effect of state blocking.

Shown in Fig. 2 are the results of the Monte Carlo simulation for the ground state recombination as a function of the initially injected carrier density, for the conditions used for the simulations good agreement was obtained in comparison with the experimental results. At the lowest injection density the carrier relaxation into the ground state is dominated by the bare sequential scattering rates with virtually no enhancement due to Auger scattering. This results in the relatively slow rise of the photoluminescence intensity. As the initial carrier density is increased Auger processes begin to play an increasingly important role so that in Figs. 2(b) and 2(c) the rise of the photoluminescence becomes increasingly more rapid. For the highest simulated excitation density the initially injected carrier density is so large that Auger enhanced scattering dominates the whole of the rise of the photoluminescence intensity.

As has been explained previously^{17,23,34} the plateau region observed in Fig. 2(c) can be explained by the effects of state blocking whereby radiative recombination occurs from a significant number of quantum dot ground states which are then rapidly reoccupied by carriers scattering down from the higher lying states.

2. Excited state recombination

We now turn our attention to the form of the photoluminescence transients arising from the excited states of the quantum dots. The photoluminescence transients shown in Fig. 3 were obtained whilst detecting at energies of 1.205, 1.277, and 1.345 eV, which correspond to the maxima in the

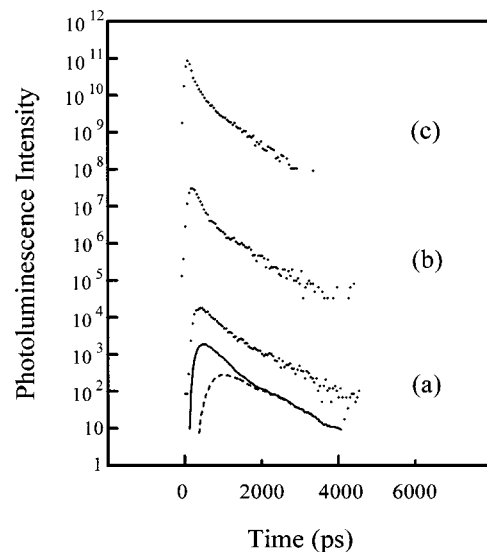


FIG. 3. The results ($\cdot \cdot \cdot$) of experimental photoluminescence time decay measurements whilst monitoring emission with energy of (a) 1.205 (first excited state emission), (b) 1.277 (second excited state emission), and (c) 1.345 eV (third excited state emission). Results of the Monte Carlo simulation for an injected reservoir carrier density of $1.3 \times 10^{12} \text{ cm}^{-2}$ of the decay (solid line) of the whole of the first excited state population and of the decay (dashed line) of the carriers in the first excited state that are prevented, at some time, from relaxing to the ground states.

highest excitation density photoluminescence spectrum [Fig. 1(c)] which involve predominantly recombination due to the first, second, and third excited states, respectively. The general form of the excited state photoluminescence transients differ greatly from those obtained for the ground state emission. In general, they exhibit a rapid rise followed by a pronounced biexponential decay, i.e., an initial fast component followed by a slower component. The lifetimes of both the fast and slow components become shorter as the index of the excited state increases. This general form of transient associated with excited state recombination has also been reported previously,^{15,27} where it was concluded that the fast decay component was associated with the decay of carriers in the excited state, but that the slow decay component was due to the decay of carriers in the ground states of smaller quantum dots which give rise to an underlying high energy tail in the photoluminescence spectrum. In this present study we can discount this explanation from the examination of the time resolved photoluminescence spectra shown in Fig. 4. The time resolved spectrum in Fig. 4(a), recorded with a time window from $t=0$ to $t=1000$ ps (a time window in which the decays are dominated by the fast component) shows recombination involving the ground state and all excited states, and is very similar to the time integrated photoluminescence spectrum shown in Fig. 1(c). When the time window is set from $t=1200$ ps to $t=3500$ ps (a temporal region dominated by the slow decay component) we still observe [Fig. 4(b)], photoluminescence from the excited states, albeit with the recombination from highest excited state slightly less intense than in Fig. 4(a) since the decay time of the slow component of the highest excited state is somewhat shorter than the time window. Therefore, the slow decay component observed when detecting at energies cor-

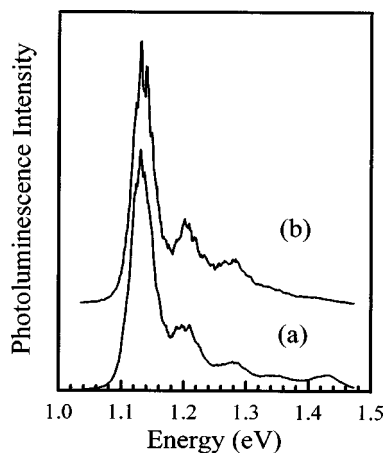


FIG. 4. Time resolved photoluminescence spectra taken using time windows of (a) $t=0 \rightarrow 1000$ ps and (b) $t=1200 \rightarrow 3500$ ps.

responding to maxima associated with the excited states emissions is due to recombination from excited state carriers and not due to some underlying contribution from the ground state recombination. This conclusion is confirmed by photoluminescence time decay measurements (not shown) obtained for the lowest excitation density where we observe only ground state photoluminescence, over the whole spectrum we measure decays with a time constant of 1.0 ns, significantly greater than the time constant associated with the slow component observed for the transients in Fig. 3. Thus, the radiative lifetime of the ground states is independent of the degree of carrier confinement, such behavior may be expected in the regime of strong confinement.^{35,36}

We can identify the origin of the two decay components shown in Fig. 3 by comparison with the temporal evolution of the excited state populations predicted by our Monte Carlo model. Again we emphasize that one advantage of a Monte Carlo simulation is that the quantum dots that have different degrees of carrier occupation are distinguishable in a randomly occupied system. Therefore, a distinction can be made between the carriers which are free to relax down to a lower unoccupied state, and those where the relaxation is blocked due to the next lowest energy state being fully occupied. On the basis of the arguments presented later we believe that these two distinct carrier populations are, in general, responsible for the biexponential behavior.

In Fig. 3 we show, along with the experimentally observed transient of the first excited state, a simulation (carrier density in reservoir of $1.3 \times 10^{12} \text{ cm}^{-2}$) of the decay of the **whole** of the first excited state population (solid line). In addition the decay of those carriers in the first excited state that are prevented, at some time, from relaxing to the ground state due to that state being fully occupied is given by the dashed line. It can clearly be seen that the time constant associated with the slow decay component is in good agreement with that of carriers subject to state blocking effects. Based on the realistic assumption that the number of carriers in the excited states is not greater than the number of carriers in the ground state, we can say that in the limiting case of carrier scattering from the first excited state to the ground state being faster than the radiative decay from the ground

state, and there being no radiative loss from the excited states, the slow excited state decay component would have a lifetime identical to that of the ground state. In other words under these circumstances the ground state radiative decay becomes the rate limiting mechanism for the excited state carrier decay, and so the excited state photoluminescence decay rate would tend toward that of the ground state. However, in practice, it is important to note that there is also a parallel radiative loss from the excited states and so the slow decay component is not solely the blocked scattering rate but a parallel combination of both carrier scattering and radiative loss. Assuming that the scattering rate between the first excited states and the ground states is greater than the first excited state radiative decay rate (this is reasonable when we consider the relatively low intensity of the photoluminescence from the first excited state), we can describe the decay of the population of the first excited state by the following rate equation

$$\frac{1}{\tau_{2(\text{meas})}} = \frac{1}{\tau_{1(\text{rad})}} + \frac{1}{\tau_{2(\text{rad})}},$$

where $\tau_{2(\text{meas})}$ is the experimentally measured decay time of the slow component of the excited state, $\tau_{1(\text{rad})}$ is the radiative decay time of the ground state, and $\tau_{2(\text{rad})}$ is the radiative decay time of the excited state. Using a slow decay component lifetime $\tau_{2(\text{meas})} = 790$ ps and a ground state radiative lifetime $\tau_{1(\text{rad})} = 1.0$ ns, the radiative lifetime of the first excited state is calculated to be 3.7 ns. An increased radiative lifetime for the first excited state compared to that of the ground state is in agreement with the recent results of Wang, Kim, and Zunger.³⁷ We cannot extend this argument to derive the radiative lifetimes of the higher excited states because, as discussed later, there is evidence that carriers in the second and third excited states do not always scatter to the next lowest energy state. Hence, the accuracy of the radiative lifetimes used in the model for the second and third excited states, 1.6 and 1.2 ns, respectively, is not high and only limited physical significance can be placed on these values.

As discussed by Heitz *et al.*¹⁵ a major factor which determines the time constant of the initial fast decay transient of the first excited state (see Fig. 3) is the scattering rate of carriers into ground states where the relaxation is not blocked due to state filling. Although the time constant of this fast component is indeed strongly influenced by the probability of scattering between the first excited states and the ground states it also includes contributions from the scattering rate of carriers from the second excited state and the first excited state radiative decay rate. Therefore, the rate equation governing the slow decay component is not applicable for the fast decay component.

As can be seen in Fig. 3 the total transient for the first excited state given by the Monte Carlo simulation is in good agreement with the experimental result, however, again we emphasize that we have only considered sequential scattering between the states. The result of modeling the decay of the second excited state using the same reservoir carrier density ($1.3 \times 10^{12} \text{ cm}^{-2}$) is shown by the solid line in Fig. 5(b). For these conditions only a single exponential decay is observed which is in good agreement with the initial fast component

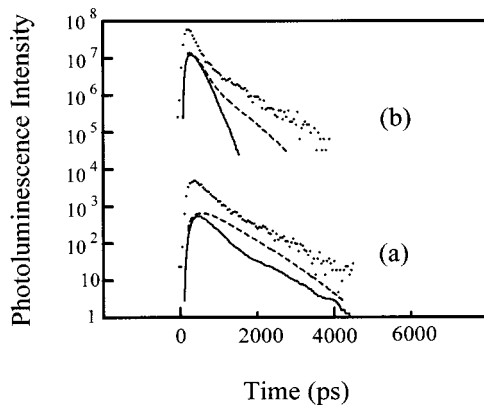


FIG. 5. Experimental data ($\cdot \cdot \cdot$) and results of the Monte Carlo simulation for decay of (a) the first excited states and (b) the second excited states for injected reservoir carrier densities of $1.3 \times 10^{12} \text{ cm}^{-2}$ (continuous line) and $3.0 \times 10^{14} \text{ cm}^{-2}$ (dashed line).

of the experimentally measured decay. However, the biexponential behavior of the measured data is not reproduced using these initial conditions. One possible explanation for this discrepancy is that for the injected carrier density used there are insufficient carriers in the first excited state to produce a reduction in the scattering rate due to state blocking. One way of producing an agreement between the measured and simulated decay of the second excited state is to increase the density of injected carriers in the Monte Carlo simulation. The results of such a calculation are shown by the dashed line in Fig. 5(b) which have been performed for a higher initial carrier density of $3.0 \times 10^{14} \text{ cm}^{-2}$. Although there is now good agreement between the simulated and measured transients from the second excited state the predicted decay of the first excited state population is no longer in good agreement with the experimentally measured transient in that the biexponential behavior has been lost. As might be expected, the simulated decay of the first excited state is now totally dominated by the state blocking induced slow component due to a very large occupation factor of the ground states [see Fig. 5(a)]. This behavior leads us to believe that the choice of the injected carrier density used in the simulation is not the cause of the discrepancy between theory and experiment. In addition it should be noted that while the carrier density required by the simulation to produce good agreement between the measured and predicted decay of the second excited state is comparable with the experimental photon excitation density this is not really a meaningful comparison. Due to the effects of nonradiative and radiative recombination of electron-hole pairs in the GaAs and the wetting layer not every photo-excited electron hole pair is captured by the quantum dots thus it is very likely that the injected carrier density in the simulation is considerably in excess of that achieved experimentally. These conclusions suggest that our model needs to be modified, to account for the observed behavior of the excited state transients.

In the regime of high density excitation the ground states are rapidly occupied thus if we propose that the biexponential behavior of the second and third excited state decay is due to state blocking involving the ground states then we have to invoke the process of nonsequential scattering. By

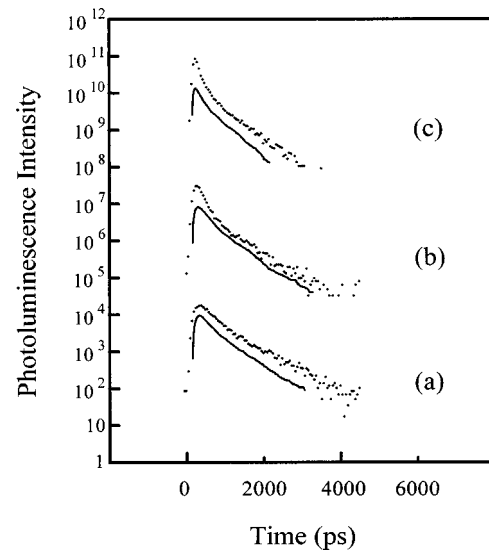


FIG. 6. Experimental data ($\cdot \cdot \cdot$) and results of the Monte Carlo simulation (solid line) including nonsequential scattering with an injected reservoir density of $1.3 \times 10^{12} \text{ cm}^{-2}$ for decay of (a) the first excited states, (b) the second excited states, and (c) the third excited states.

nonsequential we mean that carriers can scatter directly from an excited state directly down to the ground state. This will clearly allow the effects of state blocking on all the excited state decays due to the ground states being occupied to become important. This is illustrated in Fig. 6 where Monte Carlo simulations for the decay of the first, second, and third excited states where we have allowed for nonsequential scattering are shown along with the experimental results. In these simulations to achieve reasonable fits to the experimental data we have included nonsequential scattering times in the Monte Carlo model of $\tau_{4-1} = 80 \text{ ps}$, $\tau_{3-1} = 180 \text{ ps}$, and $\tau_{2-1} = 260 \text{ ps}$ and radiative lifetimes for the third, second, and first excited states of 1.4, 4.0, and 3.7 ns, respectively. The values of the radiative lifetimes used for the third and second excited states are somewhat different than those used in the sequential scattering model. This is not unreasonable as by the very nature of the purely sequential model the results of the modeling of the decays of the ground state and first excited state are relatively insensitive to the values used for the radiative lifetimes of the second and third excited states. One particular aspect of the sequential model is that it reproduces (with the parameters used) the experimentally observed progressive slow rise of the photoluminescence transients with decreasing energy of the transition. To take care of this particular aspect in the nonsequential model we have to incorporate a longer time for the capture for carriers into the second and first excited states of 550 and 1000 ps, respectively.

IV. CONCLUSIONS

In conclusion we have compared the results of the excitation density dependent photoluminescence decay experiments with the results of a Monte Carlo simulation of the decay of the four optically active states in InAs/GaAs self-organized quantum dots at 6 K. In particular we have shown that the biexponential form of the decay of the higher energy

excited state emissions can only be explained if we describe the carrier scattering processes by nonsequential interlevel scattering.

The radiative decay time measured across the whole of the spectrum of the emission from the ground states is constant with a value of 1 ns and so it can be concluded that the radiative decay rate is independent of the degree of carrier confinement for the range of quantum dots sampled.

ACKNOWLEDGMENTS

The work at UMIST is supported by a grant from the Engineering and Physical Sciences Research Council (EPSRC), UK Grant No. GR L81697. The work at Sheffield is supported by a grant from EPSRC, UK Grant No. GR/L28821. One of us (D.J.M.) acknowledges the receipt of a fellowship from EPSRC.

- ¹J. M. Moison, F. Houzay, F. Barthe, L. Leprince, E. Andre, and O. Vatel, *Appl. Phys. Lett.* **64**, 196 (1994).
- ²J.-Y. Marzin, J. M. Gerard, A. Izrael, D. Barrier, and G. Bastard, *Phys. Rev. Lett.* **73**, 716 (1994).
- ³D. Leonard, K. Pond, and P. M. Petroff, *Phys. Rev. B* **50**, 11687 (1994).
- ⁴S. Farfad, R. Leon, D. Leonard, J. L. Merz, and P. M. Petroff, *Phys. Rev. B* **52**, 5752 (1995).
- ⁵N. Carlsson, W. Seifert, A. Petersson, P. Castrillo, M.-E. Pistol, and L. Samuelson, *Appl. Phys. Lett.* **65**, 3093 (1994).
- ⁶G. W. Bryant, *Phys. Rev. B* **37**, 8763 (1988).
- ⁷Y. Arakawa and H. Sakaki, *Appl. Phys. Lett.* **40**, 939 (1982).
- ⁸M. Asada, Y. Miyamoto, and Y. Suematsu, *IEEE J. Quantum Electron.* **QE-22**, 1915 (1986).
- ⁹Y. Arakawa and A. Yariv, *IEEE J. Quantum Electron.* **QE-22**, 1887 (1986).
- ¹⁰H. Benisty, C. M. Sotomayor-Torres, and C. Weisbuch, *Phys. Rev. B* **44**, 10945 (1991).
- ¹¹S. Farfad, D. Leonard, J. L. Merz, and P. M. Petroff, *Appl. Phys. Lett.* **65**, 1388 (1994).
- ¹²M. J. Steer *et al.*, *Phys. Rev. B* **54**, 17738 (1996).
- ¹³D. Bimberg *et al.*, *Jpn. J. Appl. Phys., Part 1* **35**, 1311 (1996).
- ¹⁴Q. Xie, A. Kalburge, P. Chen, and A. Madhukar, *IEEE Photonics Technol. Lett.* **8**, 965 (1996).
- ¹⁵R. Heitz, M. Grundmann, N. N. Ledentsov, A. Hoffman, D. Bimberg, V. M. Ustinov, P. S. Kop'ev, and Zh. I. Alferov, *Phys. Rev. B* **56**, 10435 (1997).
- ¹⁶F. Adler, M. Geiger, A. Bauknecht, F. Scholz, H. Schweizer, M. H. Pikhun, B. Ohnesorge, and A. Forchel, *J. Appl. Phys.* **80**, 4019 (1996).
- ¹⁷S. Grosse, J. H. H. Sandmann, G. von Plessen, J. Feldmann, H. Lipsanen, M. Sopanen, J. Tulkki, and J. Ahopelto, *Phys. Rev. B* **55**, 4473 (1997).
- ¹⁸F. Bogani, L. Carraresi, R. Mattolini, M. Colocci, A. Basacchi, and S. Franchi, *Solid-State Electron.* **40**, 363 (1996).
- ¹⁹M. Grundmann, N. N. Ledentsov, O. Stier, D. Bimberg, V. M. Ustinov, P. S. Kop'ev, and Zh. I. Alferov, *Appl. Phys. Lett.* **68**, 979 (1996); M. Grundmann, N. N. Ledentsov, O. Stier, J. Bohrer, D. Bimberg, V. M. Ustinov, P. S. Kop'ev, and Zh. I. Alferov, *Phys. Rev. B* **53**, 10509 (1996).
- ²⁰M. Grundmann, O. Stier, and D. Bimberg, *Phys. Rev. B* **52**, 11969 (1995).
- ²¹F. Adler, M. Geiger, A. Bauknecht, D. Haase, P. Ernst, A. Domen, F. Scholz, and H. Schweizer, *J. Appl. Phys.* **83**, 1631 (1998).
- ²²A. V. Uskov, J. McInerney, F. Adler, H. Schweizer, and M. H. Pikhun, *Appl. Phys. Lett.* **72**, 58 (1998).
- ²³U. Bocklemann, W. Heller, A. Filoramo, and Ph. Roussignol, *Phys. Rev. B* **55**, 4456 (1997).
- ²⁴U. Bocklemann and T. Egeler, *Phys. Rev. B* **46**, 15574 (1992).
- ²⁵T. Inoshita and H. Sakaki, *Phys. Rev. B* **46**, 7260 (1992).
- ²⁶R. Heitz *et al.*, *Appl. Phys. Lett.* **68**, 361 (1996).
- ²⁷H. Yu, S. Lycett, C. Roberts, and R. Murray, *Appl. Phys. Lett.* **69**, 4087 (1996).
- ²⁸J. H. H. Sandmann, G. von Plessen, J. Feldmann, G. Hayes, R. Philips, H. Lipsanen, M. Sopanen, and J. Ahopelto, *Solid State Commun.* (to be published).
- ²⁹M. Vollmer, E. J. Mayer, W. W. Ruhle, A. Kutenbach, and K. Eberl, *Phys. Rev. B* **54**, R17292 (1996).
- ³⁰R. Heitz, A. Kalburge, Q. Xie, M. Grundmann, P. Chen, A. Hoffman, A. Madhukar, and D. Bimberg, *Phys. Rev. B* **57**, 9050 (1998); M. Grundmann, R. Heitz, D. Bimberg, J. H. H. Sandmann, and J. Feldmann, *Phys. Status Solidi B* **203**, 121 (1997).
- ³¹M. Grundmann and D. Bimberg, *Phys. Rev. B* **55**, 9740 (1997).
- ³²A. V. Uskov, F. Adler, H. Schweizer, and M. H. Pikhun, *J. Appl. Phys.* **81**, 7895 (1997); J. M. Gerard, J. Y. Marzin, G. Zimmermann, A. Ponchet, O. Calbrol, D. Barrier, B. Jusserand, and B. Sermage, *Solid-State Electron.* **40**, 807 (1996).
- ³³I. E. Itskevich *et al.*, *Proc. ICPS 24* (to be published).
- ³⁴S. Raymond *et al.*, *Superlattices Microstruct.* **21**, 541 (1997).
- ³⁵E. Hanamura, *Phys. Rev. B* **37**, 1273 (1988).
- ³⁶M. Sugawara, *Phys. Rev. B* **51**, 10743 (1995).
- ³⁷L. W. Wang, J. Kim, and A. Zunger, *Phys. Rev. B* (to be published).